Catalytic performance and structural properties of the Fe-FeOx system on the gas phase hydrodeoxygenation reaction of acetone

Key-words: Hydrodeoxygenation, Iron oxide, Nanomaterials.

Authors:

Pedro Becchelli de Moraes Nunes, IQ/Unicamp

Guilherme Boenny Strapasson, IQ/Unicamp

Profª. Drª. Daniela Zanchet (advisor), IQ/Unicamp

INTRODUCTION

Over the next two decades, it is anticipated that the electricity generation will surge by 52% compared to the present levels, equivalent to an extra of 16 billion tons of oil. This immense growth underscores the indispensability of adopting alternative, often renewable, energy sources [1,2,3]. Among the most well-known alternative sources is the utilization and recovery of lignocellulosic biomass to produce biofuels [4,5]. An effective method for this recovery is rapid pyrolysis, which efficiently generates bio-oil — a complex mixture of oxygenated compounds. This bio-oil holds the potential to replace diesel or gasoline derived from petroleum[6]. However, there are challenges to address, such as the physicochemical characteristics and instability of the mixture due to its high content of oxygenated species. As a result, this bio-oil cannot be directly utilized as a fuel. Furthermore, storing this mixture poses difficulties due to the high reactivity of the oxygenated compounds it contains.

The catalytic hydrodeoxygenation (HDO) reaction is a well-researched process for upgrading bio-oil. This reaction takes place in a hydrogen-rich atmosphere with the aid of a catalyst, resulting in reduced oxygen content by selectively cleaving C-O bonds [7]. Given the complexity of these compounds, a wide range of products can be formed, leading to multiple reaction pathways. Therefore, this study was conducted with a model molecule for the bio-oils, the acetone, once ketones might represent up to 15% of their content. Even with this small molecule, an extensive reaction scheme (Figure 1) is still present, due to the diverse range of side reactions, mechanisms, and reaction sites involved [8].

The catalysts employed for this reaction usually present various catalytic sites, such as oxygen vacancy (OVS), Lewis acid (LAS), Bronsted acid (BAS), and metallic sites (MS) [9, 10]. The availability of different catalytic sites can lead to multisite reactions, as well as the direct deoxygenation route, which occurs through OVS via the reverse Mars-van Krevelen mechanism (rMvK)[11]. It's important to note that all these reaction pathways rely on the use of a heterogeneous catalyst, and their effectiveness depends on properties such as the catalyst's nature, phase (metallic or oxidized), particle size, specific surface area, and crystalline structure.

Generally, the HDO reaction involves a bifunctional mechanism requiring both a MS for hydrogenation/dehydrogenation and an acid/oxophilic site to adsorb the -oxy compound and facilitate the HDO and hydrogenation reactions [12]. To achieve catalysts that promote the formation of deoxygenated products, reduction/oxidation pre-treatments can also be employed on reducible oxides. These treatments result in catalysts with a coexistence of oxidized and metallic phases, inducing bifunctional mechanisms.

Figure 1: Reaction scheme for acetone HDO with Fe-FeOx as catalysts. Deoxygenated products highlighted in gray, abbreviations for each major product in black (small characters). Adapted from [13]

Leite[13] explored nanometric Co_3O_4 and demonstrated that different pre-treatments led to the formation of core@shell-like particles with varying core and layer thicknesses and oxidation states. This variation significantly impacted the catalyst's exposed surface in the reaction environment, influencing the obtained products. Another promising candidate for the HDO reaction is iron oxide, which allows for the study of different oxidized (Fe_2O_3, Fe_3O_4, and FeO) and metallic (Fe) phases, as well as understanding their coexistence in the same particle.

In this project, the effects of the metallic and oxidized phases of iron on the HDO reaction of acetone, a model molecule representing oxygenated derivatives with ketone groups from biomass, were evaluated. Various phases of iron were obtained through thermal treatments in reducing and oxidizing atmospheres, using commercial nanometric iron (III) oxide (Fe_2O_3) as the precursor. The structural properties of these materials were characterized and correlated with the catalytic data.

METHODOLOGY

Commercial nanometric (particle size <50 nm) γ-iron(III) oxide (Fe_2O_3) acted as the initial HDO catalyst. In order to modify the catalyst's nature between its oxidized and metallic phases, different heat pretreatments were applied, such as reduction and oxidation of the precursor, using, respectively, reducing (H_2) and oxidizing (synthetic air) atmospheres at different temperature levels. As a means to avoid a heterogeneous bed in the reactor due to the extensive sintering of the iron catalyst, the oxide was reduced in batch, then ground with mortar and pestle, and later reduced again just before the reaction.

Reduction pretreatments consisted, in all cases, in an atmosphere of 30 ml/min H_2 and 70 ml/min He, with temperatures set in 550ºC (823 K), for 1 hour. Calcination was done with 50 ml/min synthetic air (that is, 10 ml/min O_2), at different temperatures (200ºC, 350ºC and 500ºC), for 2 hours. It's worth noting that the reduction temperatures of Fe_2O_3 were determined via H_2-TPR, while the max. oxidation temperature of 500ºC was determined by a bibliography TPO[14]. 600 mg of Fe was present in each sample, resulting in a WHSV of about 0.9 h⁻¹.

Regarding the HDO conditions, a 20 ml/min flow of He passed through a saturator containing acetone, dragging approximately 3.6 ml/min of it towards the reaction bed. A 76.4 ml/min flow of H_2 was also applied to the reaction medium, maintaining a proportion of approximately 21 mol of H_2 to 1 mol of acetone. The reactions were carried out at 300ºC for 3h, which was determined after screenings in temperatures ranging from 100ºC to 400ºC. Both the pretreatments and the catalytic reaction were conducted in a continuous tubular quartz reactor, in a bed of quartz wool.

Following the tests, the identification and quantification of the HDO products happened by GC/FID (gas chromatography by flame ionization analysis), while the post-reaction catalysts underwent a series of XRD analysis that will be discussed later on. Surface area determination by BET (Brunauer–Emmett–Teller theory) was attempted too.

Once the compounds were quantified, the products were distributed in order to compare their selectivity according to each sample employed. Acetone conversion and carbon balance were monitored as well, with the data collected used to determine deoxygenation degree and yields for each case.

RESULTS AND DISCUSSION

The screening test with varying temperatures for the commercial Fe_2O_3 revealed a more active catalyst at 400ºC, highly selective towards hydrocarbons (95%). However, the catalytic performance of the different redox pretreatments as a function of time on stream led to similar selectivities after 3 hours on stream, majorly associated with oxygenated products, together with deactivation of the catalysts. Such rapid deactivation of the catalysts may be explained by the deposition of coke in the materials, while the similar selectivities were a signal of a reduction occurring in all the samples, due to the elevated temperatures in an excess of hydrogen, bringing them to a similar composition before said deactivation. Therefore, the following tests were set to be conducted at 300ºC.

Figure 2 shows the results of acetone HDO of the as-received, reduced and reduced/oxidized samples, with the abbreviations of each sample indicated above the respective bars. Certain stages of the time on stream were selected to better highlight the more significant changes of conversion and/or selectivity during the reaction. The as-received sample (γ - Fe_2O_3) reached about 25% conversion, more selective towards mesityl oxide (C6O, 77%), IPA (11%) and 2,6-dimethyl-4-heptanone (C9O, 7%). The same could be observed for the RedOxi 500ºC catalyst, but the conversion was smaller (~17%).
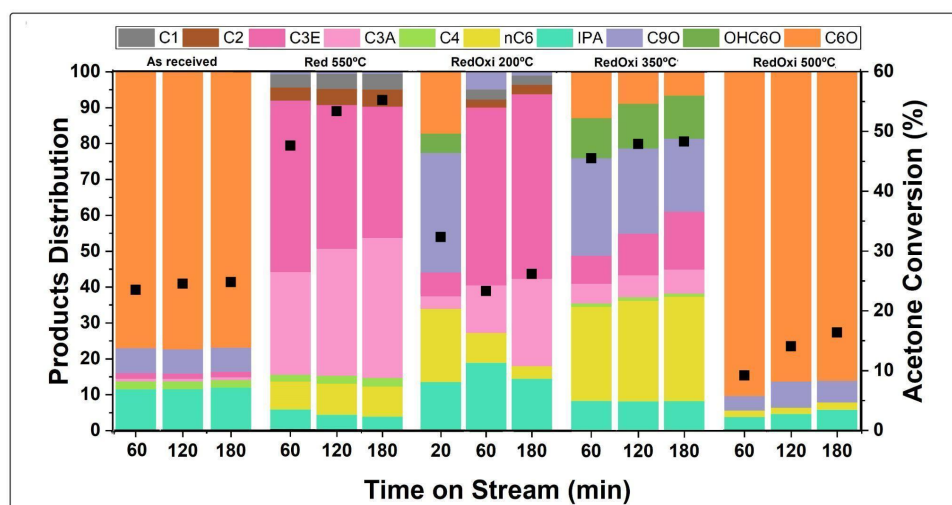
Figure 2: Products distribution (bars) and acetone conversion (squares) for the HDO reaction using different samples from the Fe-FeOx system. Selected times from the 180 minutes of time on stream.

Reducing the catalyst at 550ºC noticeably shifted both the conversion and selectivity. Propylene (C3E, conversions of 53% to 37%) and propane (C3A, conversions of 23% to 39%) were the major products, along with hexene/hexane (C6, conversions of about 8%). Acetone conversion started at 42% (20 min) and increased to 55% (180 min). RedOxi 200ºC catalyst slightly changed the profile as well, having C9O (33%), C6 (20%) and C6O (17%) as major products in the first 20 minutes. This quickly changed, however, with the selectivity shifting to C3E (49% to 51%), C3A (13% to 24%) and IPA (18% to 14%). Conversion lied at 32% for the first 20 minutes, down to 26% at the end of 3 hours on stream. RedOxi 350ºC catalyst resulted in the valorization of C6 (27% to

32%) and C9O (29% to 20%), which could indicate the coexistence of different phases and catalytic sites that favored chain growth. Conversions increased from 42% to 48% in the course of 3 hours on stream.

Moving on to the characterizations, Figure 3 gives insight to the crystal phases present in each conducted pretreatment, before and after the HDO reaction.
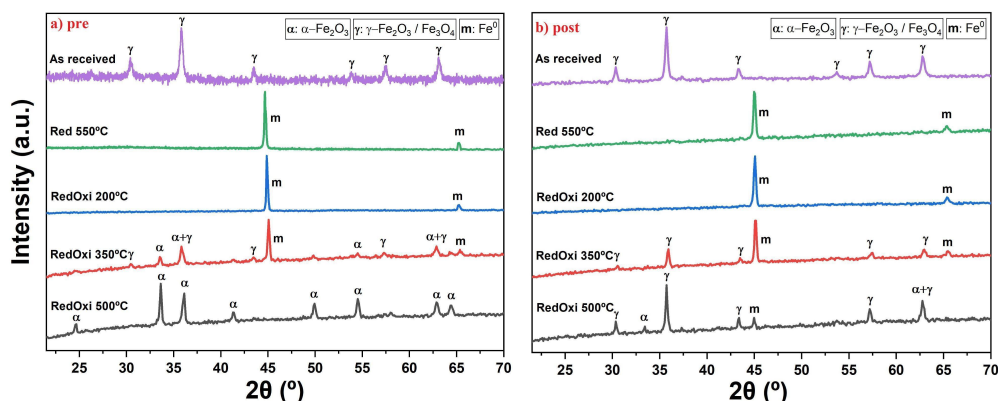
Figure 3: XRD measurements of the pre (a) and post (b) reaction samples. Peak attribution made with data collected from the ICSD crystallography database.

The as-received catalyst corresponded to the γ phase of iron(III) oxide, with no considerable changes after the reaction. Its (3 1 1) plane gives a crystallite mean size of about 21 nm, according to the Scherrer's equation. The XRD pattern of the Red 550ºC sample confirmed that the reduction to metallic iron was successful, with a crystallite mean size of 78 nm related to the (1 1 0) plane. No apparent changes were observed when comparing pre and post reaction catalysts, as well. Similarly, RedOxi 200ºC showed a predominance of the metallic phase, with a crystallite mean size of 55 nm on the same facet. When comparing this piece of data with the catalytic results, it was possible to conclude that a surface and/or amorphous oxidation could have taken place, which was probably reduced on stream due to the reaction's hydrogenating conditions. RedOxi 350ºC presented the most complex coexistence of phases of the tested samples, consisting of Fe^0 ((1 1 0) = 38 nm) and minor contributions of both γ and α Fe_2O_3 ((1 0 4) = 24 nm), which is coherent with the HDO results. The oxidized phases shifted from γ + α to just γ after reaction, due to the reducing character of the atmosphere. Finally, in the RedOxi 500ºC system, α phase was the major one, which could be explained by the thermodynamics of the media: α - Fe_2O_3 is generally the final and most oxidized phase of the iron oxides, reached preferentially at high temperatures. Pre-reaction crystallite sizes were in the range of 39.0 nm at the (1 0 4) facet. In the post-reaction sample, α mostly transitions to γ, with the surge of a reduced face happening as well. The similarities between the as-received Fe_2O_3 HDO and the RedOxi 500ºC one were coherent with the similarities of the phases presented in each of them.

Surface area determination by N_2 physisorption (BET) demonstrated that the commercial Fe_2O_3 had an estimated surface area of 97 m^2/g, while the pretreated ones resided between 5 and 10 m^2/g. Such reduction in area might be a product of the extensive sintering that took place while reducing to metallic iron.

CONCLUSIONS

A side by side comparison of the results for acetone HDO in the Fe-FeOx system makes it clear that the thermal pretreatments significantly changed both the selectivity and conversion of the catalysts, which could be attributed to the valorization or coexistence of catalytic sites in the catalyst's surface. This affirmation is in line with the presented powder diffraction patterns, which considerably differ between each other.

Correlating the obtained XRD data with the catalytic tests, some parallels could be drawn. C6O was the major product in the tests conducted with the as-received and RedOxi 500ºC samples, in which Fe_2O_3 (γ or α) was the most predominant phase. Hence, there seems to be a valorization of weak condensation acid sites with the predominance of more oxidized phases. The Red 550ºC sample was the most active and deoxygenating one, while

avoiding almost any C-C cleavage. Further testing is necessary to determine if the preferential route to propylene was the bifunctional or the OVS one, however, even if no oxidized phase was apparent in the XRD, some kind of acid site must be present to justify the great selectivity towards C3 products (possibly from surface or amorphous oxidation caused by the acetone itself). C6 was only the major product in the test carried out with the sample where most FeOx phases coexist: RedOxi 350ºC. This strongly points to the coexistence of metallic and acid sites, once both aldol condensations and deoxygenations are occurring to an extent.

REFERENCES

[1] OECD. **OECD Green Growth Studies: Energy**. Paris, 2011. 106 p. Disponível em: oecd.org/greengrowth/greening-energy/49157219.pdf.Acesso em: 30 jul. 2022.

[2] GUBAN, Dorottya; MURITALA, Ibrahim Kolawole; ROEB, Martin; SATTLER, Christian. **Assessment of sustainable high temperature hydrogen production technologies.** International Journal of Hydrogen Energy, [S. l.], v. 45, n. 49, p. 26156–26165, 2020. DOI: 10.1016/j.ijhydene.2019.08.145.

[3] CANADA'S OIL & NATURAL GAS PRODUCERS. **World Energy Needs**. 2021. Disponível em: capp.ca/energy/world-energy-needs.

[4] QIAN, Eika W.. **Pretreatment and Saccharification of Lignocellulosic Biomass**. In: TOJO, Seishu; HIRASAWA, Tadashi. Research Approaches to Sustainable Biomass Systems.Academic Press, 2014. Cap.7. p.181-204. DOI: doi.org/10.1016/B978-0-12-404609-2.00007-6.

[5] CARROLL, A., SOMERVILLE, C. **Cellulosic Biofuels.** Annual review of plant biology, 2008. 60. 165-82. 10.1146/annurev.arplant.043008.092125.

[6] MONTOYA, J. I.; CHEJNE-JANNA, F.; GARCIA-PEREZ, M. **Fast pyrolysis of biomass: A review of relevant aspects.: Part I:** Parametric study. Dyna rev.fac.nac.minas, Medellín , v. 82, n. 192, p. 239-248, Aug. 2015 . DOI: https://doi.org/10.15446/dyna.v82n192.44701

[7] MORTENSEN, P. M.; GRUNWALDT, J. D.; JENSEN, P. A.; KNUDSEN, K. G.; JENSEN, A. D. **A review of catalytic upgrading of bio-oil to engine fuels**. Applied Catalysis A: General, 2011. DOI: 10.1016/j.apcata.2011.08.046

[8] KIM, Soosan; KWON, Eilhann E.; KIM, Yong Tae; JUNG, Sungyup; KIM, Hyung Ju; HUBER, George W.; LEE, Jechan (2019). **Recent Advances in Hydrodeoxygenation of Biomass-Derived Oxygenates over Heterogeneous Catalysts**. Green Chemistry. 21. 3715–3743. 10.1039/C9GC01210A.

[9] YAN, Penghui; LI, Molly; KENNEDY, Eric; ADESINA, Adesoji; ZHAO, Guangyu; SETIAWAN, Adi; STOCKENHUBER, Michael. (2020). **The role of acid and metal sites in hydrodeoxygenation of guaiacol over Ni/Beta catalysts**. Catalysis Science & Technology. 10. 810-825. 10.1039/C9CY01970G.

[10] SUN, Junming; BAYLON, Rebecca A. L.; LIU, Changjun; MEI, Donghai; MARTIN, Kevin J.; VENKITASUBRAMANIAN, Padmesh; WANG, Yong. **Key Roles of Lewis Acid–Base Pairs on ZnxZryOz in Direct Ethanol/Acetone to Isobutene Conversion.** Journal of the American Chemical Society 2016 138 (2), 507-517 DOI: 10.1021/jacs.5b07401

[11] MIRONENKO, Alexander V.; VLACHOS, Dionisios G.; **Conjugation-Driven "Reverse Mars–van Krevelen"-Type Radical Mechanism for Low-Temperature C–O Bond Activation.** Journal of the American Chemical Society 2016 138 (26), 8104-8113 DOI: 10.1021/jacs.6b02871

[12] Teles, C.A., Rabelo-Neto, R.C., de Lima, J.R. et al. **The Effect of Metal Type on Hydrodeoxygenation of Phenol Over Silica Supported Catalysts**. Catal. Letters 146, 1848–1857 (2016). https://doi.org/10.1007/s10562-016-1815-5

[13] LEITE, D.S. **Efeito das fases metálica e oxidada do catalisador na hidrodesoxigenação de acetona**, Dissertação de mestrado, Instituto de Química - Universidade Estadual de Campinas, defendida em 21/02/2022.

[14] A Basińska, W.K Jóźwiak, J Góralski, F Domka, **The behaviour of Ru/Fe2O3 catalysts and Fe2O3 supports in the TPR and TPO conditions**, Applied Catalysis A: General, Vol. 190, 1–2, 2000, 107-115.